NUCLEAR PHYSICS A

Nuclear Physics A 584 (1995) 675–703

The inner boundary of a neutron-star crust

C.J. Pethick [a,b], D.G. Ravenhall [a], C.P. Lorenz [a,1]

[a] *Department of Physics, University of Illinois at Urbana-Champaign, 1110 West Green Street, Urbana, IL 61801, USA*

[b] *Nordita, Blegdamsvej 17, DK-2100 Copenhagen Ø, Denmark*

Received 4 August 1994; revised 12 October 1994

ELSEVIER

NOTE TO AUTHORS

Contributions (hard-copy) to Nuclear Physics A should be sent in triplicate to: Editorial Office of Nuclear Physics A, Matrix Building, Science Center WCW, Kruislaan 419, 1098 VA Amsterdam, The Netherlands; telephone: +31 20 5618161; fax: +31 20 6654969; contributions available as a LaTeX file may be e-mailed to npa@jnl.nucphys.nl. They should be accompanied by a covering letter, indicating to whom further correspondence should be addressed. Please state full address, e-mail, telephone and fax numbers of the corresponding author.

All papers are subject to refereeing. Letter-type contributions and unnecessarily long papers are unacceptable. Authors should make every effort to achieve the utmost concision compatible with clarity. They should make a careful survey of the literature to ensure that papers do not duplicate previous work and that relevant existing knowledge has been taken into account. It should be realised that the criteria for refereeing are very high. **At present less than 50% of the papers submitted are immediately acceptable.** By submitting a paper for publication in Nuclear Physics A the authors imply that the material has not been published previously nor has been submitted for publication elsewhere.

The Editors and Publisher aim at the following **time schedule**: within one week of submission the author should have received acknowledgement of receipt of his manuscript. Within two months the author should have had notification of acceptance or rejection, or a request for revision. For post-acceptance desk-editorial matters, please contact

the Publisher:
Nuclear Physics A, P.O. Box 103, 1000 AC Amsterdam, The Netherlands
telephone: +31 20 4852571, fax: +31 20 4852431
e-mail: nhpnuclear@elsevier.nl

Preparation of contributions

1. Authors should take care that their contributions are written in good English.
2. The contribution should be accompanied by original figures.
3. The paper must have a short abstract in English. Experimental papers must have keywords, see below.
4. Do not mix footnotes and references.
5. The references should be listed as in the following examples for a paper [1], for a book [2], for a conference report [3], for a laboratory report or preprint [4]:

[1] G.E. Brown, V. Koch and M. Rho, Nucl. Phys. A 535 (1991) 701.
[2] A. Bohr and B.R. Mottelson, Nuclear structure, vol. 2 (Benjamin, New York, 1975) p. 316.
[3] F. Dönau and S. Frauendorf, Proc. Conf. on high angular momentum properties of nuclei, Oak Ridge, 1982, ed. N.R. Johnson (Harwood Academic, New York, 1983) p. 143.
[4] K.G. Boyer, Ph.D. thesis, Los Alamos National Laboratory report LA-9974-T (1983).

6. Use the metric systems of units and abbreviations recommended by the SUN commission of the IUPAP, Physica A 93 (1978) 1.

Keyword abstracts. Keywords are designed to tell a reader what results are reported in an article and what the authors have concluded from these results. They enable other users to retrieve references to your articles based on indexed subjects determined by the keywords.

Keyword abstracts are coded into a bibliographic data base (Nuclear Structure Reference File) maintained at the National Nuclear Data Center, Brookhaven National Laboratory, Upton, NY 11973, USA. Four-monthly retrievals from this data base are periodically published in the Nuclear Data Sheets under the title Recent References. Information from this data base is accessible via the RECON System to scientists in the USA and Canada or may also be obtained by addressing a request to the National Nuclear Data Center.

Manuscripts. Manuscripts should be clearly typed on one side of the paper only, with wide margins and double spacing.

Continued on page 3 of cover

US mailing notice – Nuclear Physics A (ISSN 0375-9474) is published weekly by Elsevier Science B.V., Molenwerf 1, Postbus 211, 1000 AE Amsterdam. Annual subscription price (valid in North, Central and South America only) US $4792 (subject to change), including air speed delivery. Second class postage paid at Jamaica, NY 11431.

USA POSTMASTERS: Send address changes to Nuclear Physics A, Publications Expediting, Inc., 200 Meacham Avenue, Elmont, NY 11003. Airfreight and mailing in the USA by Publications Expediting.

Published weekly

Printed in the Netherlands

ELSEVIER

Nuclear Physics A 584 (1995) 675–703

NUCLEAR PHYSICS A

The inner boundary of a neutron-star crust

C.J. Pethick [a,b], D.G. Ravenhall [a], C.P. Lorenz [a,1]

[a] *Department of Physics, University of Illinois at Urbana-Champaign, 1110 West Green Street, Urbana, IL 61801, USA*

[b] *Nordita, Blegdamsvej 17, DK-2100 Copenhagen Ø, Denmark*

Received 4 August 1994; revised 12 October 1994

Abstract

The phase boundary between the liquid matter of the interior of a neutron star and the solid matter that comprises the crust is studied. The matter is assumed to consist of electrons and non-relativistic neutrons and protons in beta equilibrium. The characteristic used to identify the phase boundary is the onset of instability of the uniform matter against proton clustering, and it is examined for four interactions either used previously in astrophysical studies – Skyrme 1′, SkM and FPS – or proposed here as an improvement – FPS21. The relationship of this important property of neutron-star matter to the neutron-matter character of each interaction is explored. Characteristic densities associated with proton drip and with the liquid-gas boundary of one- and two-fluid models of the matter are compared with the instability density. Properties of some other effective interactions, relativistic and non-relativistic, are compared with those of the interactions discussed. The desirability of more calculations of neutron-matter properties, and of the utilization of those that do exist when formulating dense-matter equations of state, is emphasized. For the improved interaction FPS21, the crust fraction of the moment of inertia of a neutron star is estimated.

1. Introduction

The crust of a neutron star is important for a number of observable properties of the star. For example, neutrino emission from the crust could play an important role in the thermal evolution of the star if neutrino emission from the core was suppressed by superfluidity. Also in models of glitches that invoke coupling between the superfluid in the crust of a neutron star and a solid crust, the moments of inertia of the various

[1] Present address: Parkland College, Champaign, IL 61821, USA.

SSDI 0375-9474(94)00506-0

components of matter in the crust play a crucial role (see for example Ref. [1]). In determining the crustal properties the inner part of the crust close to the transition to the uniform matter in the core is of utmost importance, since because of the large density gradient it is this region where most of the crustal matter resides. This indicates the need to understand well the crust–core transition region.

In the past there have been many studies of the nuclei in neutron-star crusts, and the transition to the uniform phase [2–6]. The earliest works [2,3] were based on the use of the semiempirical mass formula to estimate the masses of the nuclei, together with an expression for the energy of the neutron gas outside nuclei calculated from many-body theory and the neutron–neutron interaction. These led to rather low densities for the transition between the nuclear phase and the uniform one. In the case of Ref. [2], which employed the Levinger–Simmons interaction [7], the density was about 0.3 times the nuclear density, or just above 5×10^{13} g·cm^{-3}. The work of Bethe et al. [3], which employed Nemeth and Sprung's [8] calculations of the energy of neutron matter from Brueckner–Bethe theory and the Reid interaction, gave a slightly smaller density, but, as mentioned in the "Note added in proof" [3], there were indications that if improved calculations of the neutron gas energy density were used, the transition density would be higher. In both these works the transition was found to be relatively sharp.

One of the major differences between the work of Ref. [4] and the previous ones was that the energy of nuclear matter in nuclei and the energy of the neutron matter outside were evaluated from one and the same expression for the energy density as a function of neutron and proton densities, a feature also built into the work of Refs. [5,6]. In Ref. [4], the transition density was found to be close to the saturation density of symmetric nuclear matter, $n_s = 2.7 \times 10^{14}$ g·cm^{-3}, while in Refs. [5,6] it was about 1.5×10^{14} g·cm^{-3}, or just over half the saturation density. We note that Arponen [5] stressed the importance for the transition density of the detailed form of the energy density of nuclear matter at low proton concentrations, and pointed to the differences between his results, which were based on theoretical expressions for the energy based on analytic forms of the nucleon–nucleon G-matrix, and those of BBP [4], which employed an interpolation formula fitted to theoretical results for pure neutron matter and empirical properties of nuclei close to the valley of beta stability. Another difference between the results of Refs. [2,3] and those of Refs. [4–6] is that in the latter group, the transition was found to be relatively smooth. This was in part due to the consistent treatment of matter inside and outside nuclei, and partly to the allowance for the reduction in dense neutron-rich matter of nuclear surface and Coulomb energies.

The most recent development is the discovery [9,10] that in a large fraction of the crustal matter, nuclei may be rod-like or plate-like, rather than roughly round, as they are in the laboratory. In most cases the boundary between crustal matter and the uniform phase has been determined by comparing energies of the two phases. Such calculations are complicated, partly because of the many equilibrium conditions that must be satisfied, and partly because one requires reliable estimates for the energy of an interface between nuclear matter and neutron matter in equilibrium. For nuclear matter with proton concentrations as low as those encountered in nuclei near the boundary with

the uniform phase, $\sim 10\%$ or less, the interfacial energy is very small, and thus great care is needed in estimating it.

In this paper we adopt two other approaches to estimating the location of the boundary between crust and core. We consider starting in the uniform matter in the core and reducing the density until matter becomes unstable to formation of a small periodic density modulation. This has previously been done in Refs. [4,11]. Were the transition a second-order one, this calculation would give the density of the transition. However, on general grounds, the transition must be a first-order one, and consequently some phase with a finite-amplitude density modulation will become energetically favorable compared with the uniform phase at a higher density than that at which the second-order phase transition would have occurred. Thus the density at which the second-order transition would occur gives a lower bound on the density at which the crust–core transition actually occurs. Since the crust–core transition is weakly first order, this lower bound is in fact rather close to the actual transition density, as our calculations will confirm.

The second approach is to study the phase equilibria between different sorts of nuclear and neutron matter in bulk, neglecting Coulomb and surface effects. This will underestimate the energy of inhomogeneous phases, and will therefore give an upper limit to the maximum density at which inhomogeneous phases are energetically preferred relative to the uniform phase.

This paper is organized as follows: Section 2 describes the basic formalism for examining the instability to proton clustering, and in Section 3 we give instability results for the FPS21 interaction. In Section 4 we introduce and contrast the four nuclear interactions of which we make a detailed study. In Section 5 we compare their instability predictions, and explore what particular aspects of the nuclear interaction are important for determining the crust–core transition. We emphasize their neutron-matter predictions, in comparison with ab initio calculations of that quantity. The comparison of instability density and the densities of the actual first-order phase transition between spherical bubbles and uniform matter is made in Section 6 for the FPS interaction. Section 7 discusses the two-bulk-fluid to one-fluid phase transition, the onset of proton drip that is its precursor, and their relationship to the instability density. In Section 8 a wider comparison is attempted, with some very recent ab initio calculations, and with some popular relativistic and non-relativistic effective-interaction models. It is concluded that the energy of neutron matter in the density range of interest ($\lesssim 0.1$ fm^{-3}) is a rather well established property, although few effective interactions make a good fit to it. We also explore the behavior of the neutron single-particle potential dictated by the requirement that at low density the interaction energy is directly related to the neutron–neutron scattering length. This produces characteristics that are mimicked by the FPS21 interaction. The resulting single-particle potential is roughly independent of density for a range of densities, and this could have consequences for calculations of halo nuclei. In the conclusion the instability results for FPS21 are summarized and related to the neutron-star moment of inertia crust fraction. An appendix gives algebraic results for the Skyrme and generalized Skyrme interactions.

2. Basic formalism

We begin by calculating the energy change when small sinusoidal variations of the particle densities are imposed on a uniform liquid of protons, neutrons and electrons. To second order in the density modulations, $\delta n_{\boldsymbol{q}}^{i}$, the energy density may be written as

$$E - E_{\mathrm{U}} = \frac{1}{2}\sum_{\boldsymbol{q}}\sum_{i,j}\frac{\delta^2 E}{\delta n_i(\boldsymbol{q})\delta n_j(\boldsymbol{q})^*}\delta n_i(\boldsymbol{q})\delta n_j(\boldsymbol{q})^*, \tag{1}$$

where E_{U} is the energy of the uniform phase, and the subscripts i and j denote the particle species. The first-order terms in the expansion vanish because there is no net change in the number of particles of any species. The matrix has the form

$$\frac{\delta^2 E}{\delta n_i(\boldsymbol{q})\delta n_j(\boldsymbol{q})^*} = \begin{pmatrix} \dfrac{\partial\mu_{\mathrm{p}}}{\partial n_{\mathrm{p}}} + D_{\mathrm{pp}}q^2 + \dfrac{4\pi e^2}{q^2} & \dfrac{\partial\mu_{\mathrm{p}}}{\partial n_{\mathrm{n}}} + D_{\mathrm{pn}}q^2 & -\dfrac{4\pi e^2}{q^2} \\ \dfrac{\partial\mu_{\mathrm{p}}}{\partial n_{\mathrm{n}}} + D_{\mathrm{pn}}q^2 & \dfrac{\partial\mu_{\mathrm{n}}}{\partial n_{\mathrm{n}}} + D_{\mathrm{nn}}q^2 & 0 \\ -\dfrac{4\pi e^2}{q^2} & 0 & \dfrac{\partial\mu_{\mathrm{e}}}{\partial n_{\mathrm{e}}} + D_{\mathrm{ee}}q^2 + \dfrac{4\pi e^2}{q^2} \end{pmatrix}. \tag{2}$$

Here $4\pi e^2/q^2$ is the Coulomb interaction, and the coefficients D_{ij} determine the terms in the energy functional proportional to gradients of the particle densities. Note that $D_{ij} = 2B_{ij}$ in the notation of Ref. [4].

For the system to be stable to small density modulations, all eigenvalues of the matrix must be positive. A necessary and sufficient condition that a hermitian matrix has positive eigenvalues [12] is that a number of minors of the determinant be positive:

$$a_{11} \geqslant 0, \qquad \begin{vmatrix} a_{11} & a_{12} \\ a_{21} & a_{22} \end{vmatrix} \geqslant 0, \qquad \ldots \qquad \begin{vmatrix} a_{11} & a_{12} & \cdots & a_{1n} \\ a_{21} & a_{22} & \cdots & a_{2n} \\ \cdots & \cdots & \cdots & \cdots \\ a_{n1} & a_{n2} & \cdots & a_{nn} \end{vmatrix} \geqslant 0. \tag{3}$$

In the case of the problem under consideration, the first condition corresponds to the requirement that the system be stable with respect to small modulations of the proton density, and the second is a requirement for simultaneous modulations of proton and neutron densities. The final condition involves modulation of all three densities.

For all of the nuclear interactions we have employed, the diagonal terms of the matrix are positive. The most stringent condition for stability is then the requirement that the determinant of the whole matrix be positive, since the determinant of the 2×2 neutron–proton part of the matrix is always greater than the determinant of the whole matrix.

The condition that the determinant be positive may be written as

$$v(q) = \left(\frac{\partial\mu_{\mathrm{p}}}{\partial n_{\mathrm{p}}} + D_{\mathrm{pp}}q^2 + \frac{4\pi e^2}{q^2}\right) - \frac{\left(\partial\mu_{\mathrm{p}}/\partial n_{\mathrm{n}} + D_{\mathrm{pn}}q^2\right)^2}{\partial\mu_{\mathrm{n}}/\partial n_{\mathrm{n}} + D_{\mathrm{nn}}q^2}$$

$$-\frac{\left(4\pi e^2/q^2\right)^2}{\partial\mu_e/\partial n_e + D_{ee}q^2 + 4\pi e^2/q^2} > 0. \tag{4}$$

In this form, $v(q)$ is the coefficient of $(\delta n_p(\boldsymbol{q}))^2$ in (2), and represents the tendency to stability of the protons: the terms in the first bracket are the nuclear bulk, density gradient, and Coulomb contributions to the direct interaction of the proton modulations. The second and third terms are the induced effects due to the interactions of the proton modulations with those of the neutrons and the electrons, respectively. Approximations to these latter terms obtained by neglecting D_{ee} and all but the lowest powers of D_{nn} and D_{np} bring these terms into the form discussed by BBP [4]:

$$v(q) \simeq v_0 + \beta q^2 + \frac{4\pi e^2}{q^2 + k_{TF}^2}, \tag{5}$$

where

$$v_0 = \frac{\partial\mu_p}{\partial n_p} - \frac{\left(\partial\mu_p/\partial n_n\right)^2}{\partial\mu_n/\partial n_n} = \left(\frac{\partial\mu_p}{\partial n_p}\right)_{\mu_n,\mu_e}, \tag{6}$$

$$\beta = D_{pp} + 2D_{np}\zeta + D_{nn}\zeta^2, \qquad \zeta = -\frac{\partial\mu_p/\partial n_n}{\partial\mu_n/\partial n_n}, \tag{7}$$

$$k_{TF}^2 = \frac{4\pi e^2}{\partial\mu_e/\partial n_e} = \frac{4\alpha}{\pi}(3\pi^2 n_e)^{1/3}. \tag{8}$$

The quantity ζ is the amplitude of the neutron modulation relative to that of the proton, and k_{TF} turns out to be the inverse of the Thomas–Fermi screening length of the electrons. In this form the gradient and Coulomb effects clearly make positive contributions to $v(q)$, thus tending towards stability. There is a minimum value $v(Q)$ at $q = Q$ that marks the least stable modulation:

$$Q^2 = \left(\frac{4\pi e^2}{\beta}\right)^{1/2} - k_{TF}^2, \qquad v(Q) = v_0 + 2(4\pi e^2\beta)^{1/2} - \beta k_{TF}^2. \tag{9}$$

In situations where k_{TF}^2 is small compared with q^2, as is the case here, the gradient and the Coulomb terms clearly make approximately equal contributions to $v(Q)$. This amplifies by a factor 2 the contribution the gradient terms make towards stability. For the uniform fluid to be stable with respect to coagulation of the protons, $v(Q)$ must be positive. The density at which this condition fails, $n(Q)$, marks the lowest nucleon density at which uniform matter is stable to small modulations of this kind.

While less revealing, the numerical minimization of the unapproximated determinant (4) is simple, and one may thus find the wavenumber for least stability without approximations. Since for the Skyrme and Skyrme-like interactions we shall examine the derivative terms, which are not the first terms of an expansion, but are a truncation that represents all of the finite-range effects, it is useful to determine the size of the difference between the two procedures (4) and (5). As we shall show, however, it is very small.

3. Stability results

Some of the ingredients in the instability analysis of the previous section are shown as a function of baryon density in Fig. 1. The matter whose properties are given consists of neutrons, protons and electrons, and is in the uniform phase in equilibrium with respect to beta decays of the form $p + e^- \rightarrow n + \nu_e$ and $n \rightarrow p + e^- + \bar{\nu}_e$. At zero temperature the condition is $\mu_n = \mu_p + \mu_e$, if one assumes that the neutrinos escape freely from the star, so that their chemical potentials may be set equal to zero. The particular interaction used, called FPS21, has the property that it is a good fit to both the nuclear and neutron-matter calculations of Friedman and Pandharipande [13]. The curve v_0 represents static stability according to (6), while the curves labelled $v_{\min}$ include the contributions from gradient and Coulomb effects, calculated either with the exact minimization of Eq. (4) or the approximate results of Eq. (5). The quantities Q^2, the values of q^2 that minimize $v(q)$ by the two methods, are also shown. One sees from the densities at which these three v curves cross the axis that gradient and Coulomb effects promote stability down to lower densities, and that the results of the BBP approximation and the exact diagonalization are virtually indistinguishable.

One deduces from Fig. 1 that with the FPS21 nuclear interaction, uniform beta-stable

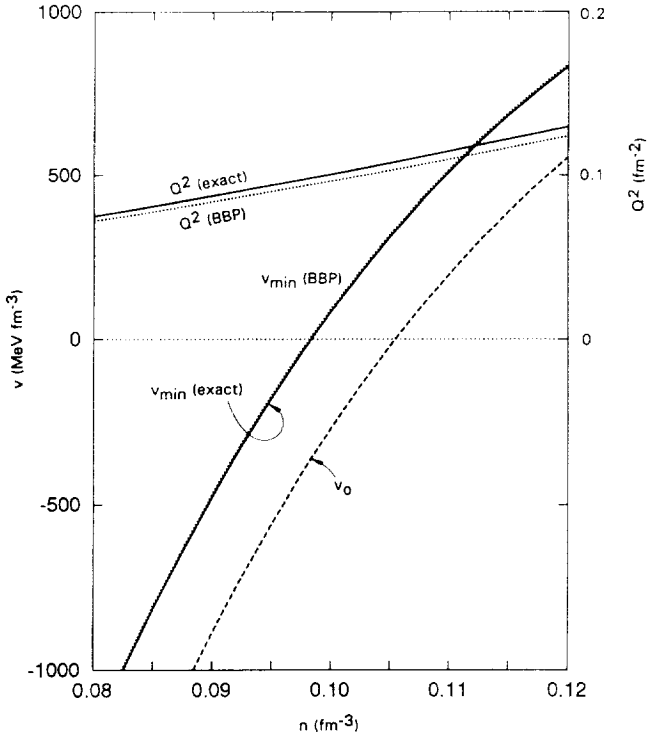

Fig. 1. The contributions to the stability criteria (4) and (5) (see text) as functions of density, for uniform matter in beta equilibrium. The interaction used here is FPS21 (see text).

matter is stable against the particular form of density modulation assumed in Section 2 down to a baryon density $\simeq 0.10$ fm^{-3}. This is an approximation to the density that marks the transition between matter in the crust of a neutron star and the uniform matter interior to it. The important questions that this result raises are: does the transition density depend on the nuclear interaction used? How is the transition density related to other nuclear properties? What is a "best guess" as to the value of this transition density?

4. Interactions

The four different interactions that have been used to explore the crust phase boundary at the level needed to distinguish phenomena such as non-spherical nuclei are all based on the Skyrme interaction (see Table 1). Before comparing their instability properties, we make some observations on the properties and limitations of this type of interaction, to motivate the generalized form we suggest, and to pinpoint further possible improvements. The relevant algebra for Skyrme interactions is given in the appendix.

4.1. Skyrme interactions

The essential simplifying property of a Skyrme interaction is that it has zero range. In momentum space, the two-nucleon t-matrix that generates the interaction is assumed to be of the general form

$$t(\boldsymbol{k}, \boldsymbol{k}') = t_0 + \tfrac{1}{2}t_1(k^2 + k'^2) + t_2\boldsymbol{k}\cdot\boldsymbol{k}' + t_3 n^{2+\alpha}, \tag{10}$$

Here $\boldsymbol{k}$ and $\boldsymbol{k}'$ are the initial and final relative momenta of a colliding pair of nucleons, and the t_1 and t_2 terms containing them are the first terms in a Taylor expansion for finite-range effects. With the assumption that the coefficients t_i are constant, this t-matrix generates in a well-known way [14] a nuclear hamiltonian in which the terms of (10) contribute simple dependences on the density n and a linear dependence on the kinetic density τ: $t_0 n^2$, $t_{1,2} n\tau$ and $t_3 n^{2+\alpha}$. The momentum-dependent terms generate also

Table 1
Densities of phase transitions, and pressure at instability

Interaction	$n(Q)$ [a] (fm^{-3})	$n_{\mathrm{p-drip}}$ [b] (fm^{-3})	$n_{1\leftrightarrow 2}$ [c] (fm^{-3})	$p[n(Q)]$ [d] ($\mathrm{MeV\cdot fm}^{-3}$)
SkM	0.0737	0.0769	0.0843	0.379
Skyrme 1′	0.0995	0.1066	0.1085	0.456
FPS	0.0957	0.1031	0.1056	0.373
FPS21	0.0983	0.1040	0.1081	0.500

[a] Onset of instability against proton clustering.
[b] Density of proton drip in the two-fluid phase.
[c] Phase transition from the two-fluid to the one-fluid phase.
[d] Pressure at the onset of instability against proton clustering.

Table 2
Parameter values of the Skyrme interactions

Model	t_0 (MeV·fm^3)	x_0	t_1 (MeV·fm^5)	t_2 (MeV·fm^5)	t_3 (MeV·fm^6)	x_3	α
1′	−1057.3	0.2885	235.9	−100.	14463.5	0.2257	1
SkM [19]	−2645.0	0.09	385.	−120.	15595.	0	$\frac{1}{6}$

a quadratic dependence on the gradient of the density. It is these gradient contributions, plus the terms from the extended Thomas–Fermi expansion of the τ_n, τ_p operators [15], that provide the curvature terms D_{ij} of Section 2.

In the detailed forms of the hamiltonians given in the appendix, the parameters of the t-matrix (10) are supplemented by spin-exchange terms, the only type of exchange contribution permitted for a zero-range interaction. Those for the potential energy, x_0 and x_3, allow adjustment of the charge-symmetry properties. The kinetic-energy exchange parameters x_1 and x_2 have the effect of decoupling to some degree the effective mass contributions to the kinetic energy from the gradient contributions to the potential energy. If x_1 and x_2 are assumed to be zero, those two parts of the nuclear effective hamiltonian are uniquely related to each other. The effective interaction (10) or its more general form (A.1) produces hamiltonians that are remarkably economical parametrizations of properties of ordinary nuclei. The interactions Skyrme 1′ and SkM are just two of many examples that exist in the literature. Skyrme 1′ and SkM each have spin exchange only in the potential energy: x_1 and x_2 are zero for both of them.

In order to extrapolate such models, which handle nuclei with proton fractions $x_p \gtrsim 0.4$, to neutron-star matter, for which $x_p \lesssim 0.1$, one uses the only information available on neutron matter, namely ab initio microscopic calculations of uniform matter from two-nucleon scattering data. Applied to uniform neutron matter, assumed to be at zero temperature, the t_i terms of Skyrme interactions contribute to the energy per baryon density dependences $t_0 n$, $t_{1,2} n^{5/3}$ and $t_3 n^{1+\alpha}$. With so few parameters, and such restricted density dependence, it is not always possible to match the "observed" neutron-matter properties closely. The Skyrme 1′ and SkM interactions are of this type, and each was matched in some way to the microscopic zero-temperature calculations of Siemens and Pandharipande [16]. Skyrme 1′ is based on the early fit to closed-shell nuclei by Vautherin and Brink [14] and, after being modified [17] to fit neutron matter [16], it has been used in dense-matter explorations by Lattimer et al. [18]. SkM was developed by Krivine, Treiner and Bohigas [19], and used in finite-temperature astrophysical applications by Bonche and Vautherin [20] and by Lassault et al. [21]. Its predictions for neutron-star crusts were studied in Ref. [10]. For completeness, the parameter values for these interactions are given in Table 2.

4.2. *Generalized Skyrme interactions*

In the generalized type of Skyrme interaction to which FPS21 belongs, the t-matrix

Table 3
Fit to nuclear and neutron matter

n	p_n
1	339 MeV^3
2	−1054 MeV·fm^3
3	89.8 MeV·fm^5
4	0.457 fm^3
5	−59.0 MeV·fm^5
6	0.284 fm^3
7	−543 MeV·fm^3
8	2316 MeV·fm^3
9	6.50 fm^3
10	1.78 MeV
11	52.0 MeV·fm^3
12	−5.50 MeV
13	−197 MeV·fm^3

coefficients in (10) are taken to be functions of density, as detailed in the appendix. They are to be fitted to the "observed" (in fact computed) temperature- and density-dependent energies per baryon of neutron and nuclear matter, in this case the more recent, finite-temperature microscopic calculations of Friedman and Pandharipande [13]. The flexibility associated with x_0 and x_3 is subsumed into the more general parametrization used for the potential terms. The two distinct functions used in the kinetic energies correspond to the two parameters t_1 and t_2 of (10), so that implicitly we assume that x_1 and x_2 are zero. Thus the gradient terms in the potential energy are uniquely determined by the effective-mass terms, which are obtained by fitting the temperature dependence of the nuclear- and neutron-matter energies. The values of the 13 parameters involved are given in Table 3. Some explorations have been made of the effect of non-zero values for x_1 and x_2, but the possibility needs further study.

An interaction of this type, FPS [22], was employed recently by Lorenz et al. [10] to explore the properties of solid neutron-star crusts. As will be seen, the FPS model is not a very close fit to the neutron-matter energies, although it was intended to be! The required modification in nuclear-matter properties, noted in Ref. [22], spoiled the original fit to neutron matter. The interaction FPS21 introduced in this work corrects that problem. The interaction FPS and the results obtained with it are still internally consistent, however, and here it provides another datum in our comparison of properties of interactions.

The terms associated with p_{10} and p_{12} in (A.3) of the appendix are needed to approximate the low-density behavior obtained in the calculations of Ref. [13]. Because of the basic role played by two-body correlations the nuclear-matter results of Ref. [13] correspond at low density to a gas of deuterons, and the proton and neutron chemical potentials obtained are in the limit of zero density finite and negative. That result arises from the p_{10} term, whose contribution to H is $\propto n$. To avoid this behavior, which is inappropriate for a nuclear hamiltonian for neutrons and protons, that term is replaced by

Table 4
Parameter values in the generalized Skyrme interactions

Model	p_{10} (MeV)	p_{11} (MeV·fm^3)	p_{12} (MeV)	p_{13} (MeV·fm^3)
Fit to FP [13]	1.78	52.0	−5.50	−197
FPS [22]	0	63.125	−5.50	−197
FPS21	0	63.125	1.62	−241.5

p_{10}/n_s, and amalgamated into p_{11}. For neutron matter, however, since there is no bound nn system, the behavior obtained by Ref. [13] should describe correctly the interacting system. The values of p_{12} and p_{13} are therefore adjusted to compensate for setting p_{10} to zero and to restore the original fit to neutron matter. To make clear what is being used, we give in Table 4 the values of the relevant parameters involved in the original fit, in the intermediate fit FPS, and in the correct fit FPS21. We return in a later section to a possible physical consequence of the p_{12} term in the FPS21 interaction. The interaction FPS describes well the ground-state energies of spherical isolated nuclei [10], and the neutron-matter adjustment involved in going to FPS21 does not affect that feature markedly. (For ^{208}Pb, the energy per baryon changes by ~ 30 keV [23].)

The basic Skyrme assumption, that the dynamic properties are determined by a two-body interaction, Eq. (10), results in a solely quadratic dependence on the nuclear charge asymmetry $(n_n - n_p)/n$ of the strong-interaction part of the nuclear hamiltonian. For definiteness, we assumed that the generalized Skyrme interactions behaved in the same way. Apart from simplicity, a partial justification for that assumption is provided by the direct calculations, by Lagaris and Pandharipande [24] of the properties of charge-asymmetric nuclear matter. They find that at a density of $n = 0.1589$ fm^{-3} the quadratic symmetry coefficient of nuclear matter is $\varepsilon_{sym} = 29.96$ MeV. The value obtained at that density with FPS21, as a result of the assumption of quadratic dependence, is 29.50 MeV, which agrees quite well with the direct calculation. The estimate in Ref. [13] of the quartic term in the charge asymmetry gives a contribution to the neutron-matter energy per baryon at that density of < 1 MeV. (This is an upper limit.) This quantity translates, however, into a contribution to μ_p in neutron matter of < 8 MeV, a $< 7\%$ modification in its value at that density. This is rather larger than is comfortable. Since μ_p and its derivatives are quantities needed for the instability calculation, it would be very reassuring to have a direct calculation of μ_p for neutron matter, as a different constraint on the charge symmetry.

5. Stability of different interactions

We show in Fig. 2 the static v_0, (6), and the exact value of v_{min} from (4), for all four of the nuclear interactions that we consider. Listed in Table 1 are the densities $n(Q)$ at which v_{min} is zero, and the pressures of the matter there. It is evident from Fig. 2 that not all of these interactions agree on the stability properties and density of the phase

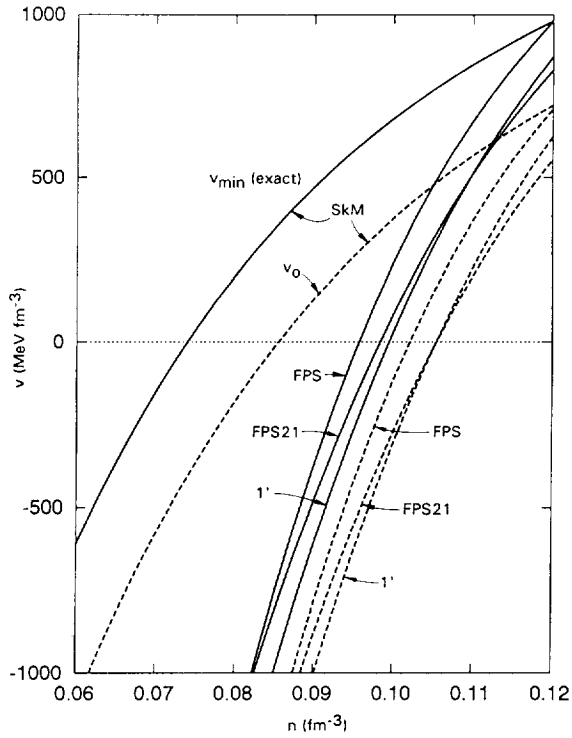

Fig. 2. The stability energy $v(Q)$, (4), and the static approximation to it, v_0, (6), as functions of density, for uniform matter in beta equilibrium, for interactions of the Skyrme type (see text). The matter is stable against proton clumping so long as $v(Q) > 0$.

transition to inhomogeneous matter. Since they each give reasonable accounts of nuclear matter and terrestrial nuclei, it is interesting to find what properties of the interacting np system they disagree on. An obvious candidate is neutron matter.

Basic to the interactions is the energy functional. Plotted in Fig. 3 as "data points" is the energy per baryon of neutron matter as given by the microscopic calculations used to locate the neutron-matter aspects of the four effective interactions. That of Siemens and Pandharipande [16] used the Reid potential, while that of Friedman and Pandharipande [13] used the V14 two-body interaction plus a three-nucleon interaction. Of the two calculations, Ref. [13] was made ten years later than Ref. [16], and superseded it both in two-nucleon input and in many-body technique.

Shown in Fig. 3 are the neutron-matter energies given by the four effective interactions we are comparing. There is clearly a progression in the quality of the agreement with the computed points of Refs. [13,16], but it is not obvious from Fig. 3 why the SkM stability prediction shown in Fig. 2 should be so different from those of Skyrme 1′, FPS and FPS21, and why those three should have such similar stability properties. We recall that the instability criteria (4) and (5) involve not the energy of the matter, but derivatives of it, in the form of chemical potentials, in fact *their* density derivatives. We

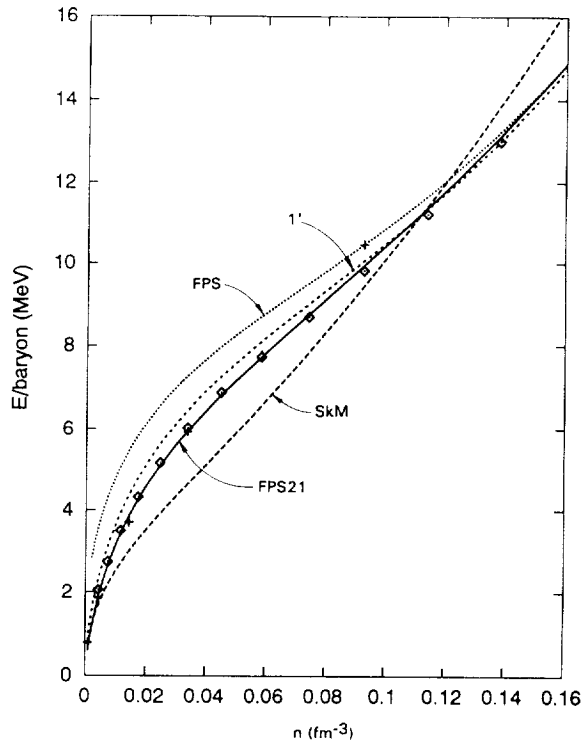

Fig. 3. The energy per baryon of uniform neutron matter as a function of density. The diamonds are the values obtained by Friedman and Pandharipande [13], the "+" signs those of Siemens and Pandharipande [16]. The interactions Skyrme 1′, SkM, FPS and FPS21 are described in the text.

examine in Fig. 4, therefore, the proton chemical potential in neutron-matter that comes from the four interactions. Included also, as points on the graph, are numerical results of Ref. [16]. One sees that there is surprising unanimity among all of the interactions, although they all give values somewhat lower than the point from Ref. [16] at $n \simeq 0.093$ fm^{-3}. The neutron chemical potentials are shown in Fig. 5. Here there appears a clear separation between SkM and the other three interactions. The value of μ_n for SkM is somewhat different for most of the density range, and clearly the derivative $\partial\mu_n/\partial n$ is distinctly larger. Also, while the FPS21 curve departs consistently from those of FPS and Skyrme 1′ at densities ~ 0.1 fm^{-3}, the *slopes* of those three curves are very similar. These facts may explain the stability results of the four interactions. We must remember, however, that the chemical potential derivatives that contribute to the static stability v_0, (6), are to be evaluated for beta-stable matter, and not for pure neutron matter. In fact, the derivative $\partial\mu_p/\partial n_p$ contains a term proportional to $n_p^{-1/3}$, and is singular for pure neutron matter.

The fact that the μ_n behavior discriminates among the four interactions, whereas that of μ_p does not, may be understood as follows: the energies of all four interactions have been fitted to nuclei along the stability line, and also, with varying precision, to

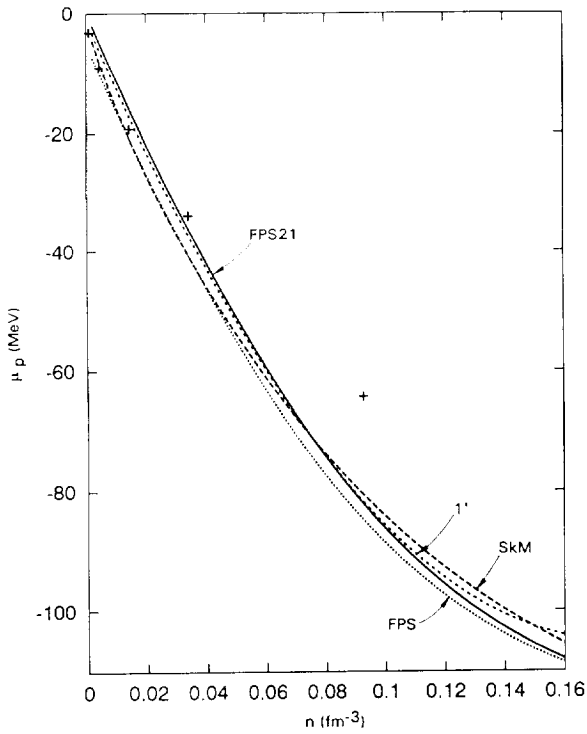

Fig. 4. The proton chemical potential of uniform neutron matter as a function of density. The "+" signs are the values obtained by Siemens and Pandharipande [16]. The interactions Skyrme 1′, SkM, FPS and FPS21 are described in the text.

the neutron-matter energies. The interpolation in the coordinate n_n–n_p between those regions is quadratic in all cases. The quantity μ_p is the slope of the parabola at $n_p = 0$, which, as a simple calculation will show, is not sensitive to the exact location of the bottom or edge of the parabola. (The fact that all curves are significantly lower than the datum of Ref. [16] at $n \simeq 0.093$ fm^{-3} is not a serious discrepancy, since by this density the energy per baryon from that reference, shown in Fig. 3, is also suspiciously high.) On the other hand, μ_n is the slope, in the n_n coordinate, of the direct fit of energies to neutron matter, and amplifies any imperfections in the fit. We can verify this distinction by examining the pressure p, as shown in Fig. 6. This is not really an independent test, since for neutron matter $p = n_n\mu_n - E$, but it is useful since Refs. [13,16] give results also for the pressure. Included in Fig. 6 are their values, and curves from the four interactions[2]. The grouping of the curves in Fig. 6, and its clear relationship to the grouping in the stability results of Fig. 2, is evident. The SkM interaction has a

[2] The interaction FPS21 was fitted to only the energy per baryon calculated in Ref. [13], and not to the pressure values also obtained there. Any lack of agreement with the Friedman–Pandharipande pressure results is a measure of the errors in the choice of functions and parameters in the fitting to their numerical values of the energy per baryon. The fit was made to the whole density range quoted by Ref. [13], $n_n \leqslant 0.83$ fm^{-3}.

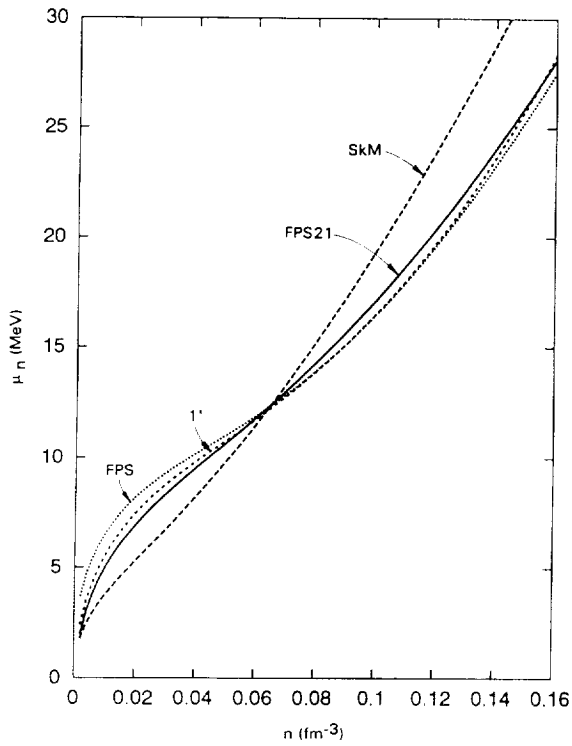

Fig. 5. The neutron chemical potential of uniform neutron matter as a function of density. The interactions Skyrme 1′, SkM, FPS and FPS21 are described in the text.

much higher pressure for neutron matter in the density region $n \sim 0.08$ fm$^{-3} \sim \frac{1}{2}n_s$. We conclude that to reproduce the thermodynamic properties of a given set of "neutron-matter data" that are important for the phase boundary, the energy functional must be fitted rather closely, in order to reproduce correctly the density derivatives of it, the quantities on which the stability depends. We return to the question of the relative immutability of μ_p, which may be due in part to the choice of isospin dependence in the effective interactions, in the discussion section.

6. Comparison with a more complete model of the solid phase

The phase transition between uniform beta-stable matter and a solid phase composed either of nuclei or of neutron-bubbles requires some model description of the solid. These models usually contain further quantities such as surface energies, etc., that are not easy to calculate. The stability analysis that we have given, based on the uniform phase, is theoretically simpler and more accessible. A comparison between the two treatments provides a useful check on our methods, nonetheless.

The interaction we have studied most extensively up to now is FPS. Although we

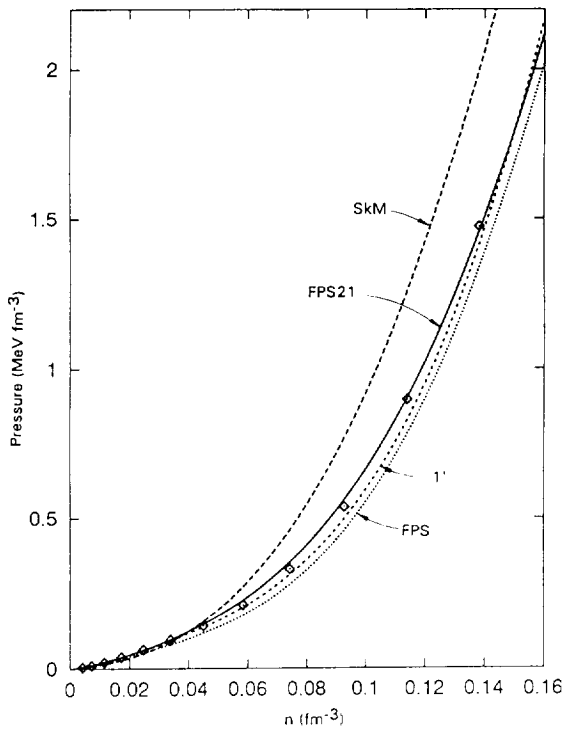

Fig. 6. The pressure of uniform neutron matter as a function of density. The diamonds are the values obtained by Friedman and Pandharipande [13] the "+" signs those of Siemens and Pandharipande [16]. The interactions Skyrme 1′, SkM, FPS and FPS21 are described in the text.

believe that FPS21 is the preferable interaction, since it is a much closer fit to neutron matter [13], the only interaction for which all of the ingredients for the full description of the solid are available for comparison is FPS. The results of a full compressible liquid drip treatment for that interaction are as follows. The energies per unit volume of the spherical bubbles phase and of the uniform phase for FPS are equal at a density of $n_e = 0.09607$ fm^{-3}. The first-order transition between these two phases, calculated by assuming equality of pressures and neutron chemical potentials, extends from a density $n_1 = 0.09473$ fm^{-3} to a density $n_2 = 0.09620$ fm^{-3}. The instability density for uniform matter for this interaction is $n(Q) = 0.09565$ fm^{-3}. As discussed in the introduction, $n(Q)$, the density phase transition would have if it were of second order, is less than n_2, the upper edge of the first-order transition density range.

It is thus clear that to an accuracy $\lesssim 0.001$ fm^{-3}, the instability density $n(Q)$ can be assumed to represent the maximum density of the solid material in the neutron-star crust.

7. The bulk equilibrium approximation

We now discuss other related densities that may be even simpler to calculate.

A simplification of the solid phase is obtained by neglecting the Coulomb and surface (i.e. density gradient) contributions to the energy. One can then calculate the properties of a phase with two uniform components, one a "nuclear fluid" consisting of neutrons and protons, the other consisting of neutrons, all in thermodynamic and beta equilibrium. Another approximation to the boundary between solid and liquid neutron-star phases is then given by the phase transition between this two-fluid phase and the uniform one-fluid phase we have discussed in the previous sections. The properties of the two-fluid phase may be exhibited on the "map of Africa" shown in Fig. 7. The interaction used there is FPS21. Isobars of nuclear pressure are plotted on the space of neutron–proton chemical potentials versus proton fraction. The vertical and horizontal dotted lines join points that have equal neutron chemical potentials (and pressures, of course), and indicate the proton chemical potentials of the two fluids. One case chosen, with pressure 0.005 MeV·fm^{-3}, is not far from neutron drip, and the proton chemical potentials for this case are far from equality, a necessary condition for the protons to be confined to the "nuclear" fluid.

Up to now we have tacitly assumed that the bulk equilibrium is between one phase with non-zero proton concentration, and pure neutron matter. However, it could happen that the proton chemical potential in the pure neutron phase fell below that in the phase with a non-zero proton concentration. It would then be energetically favorable for some protons to migrate from the proton-rich phase to the initially pure neutron phase. This corresponds to "proton drip", by analogy with the situation for neutrons at lower densities, when the most energetic occupied neutron orbitals become continuum states, rather than bound ones. We denote this density by $n_{\mathrm{p-drip}}$. At densities somewhat above that for the proton drip, matter consists of two phases with different non-zero proton concentrations in equilibrium.

With further increase in density, the energy per particle of the matter will eventually rise to that of the uniform phase. This will generally occur by one of the two phases in the two-phase equilibrium growing at the expense of the other one until it occupies all of space. Another possibility is that the proportions of two phases remain non-zero, but the two phases in equilibrium become increasingly similar, and eventually indistinguishable. This latter possibility will be realized only for very specific conditions, such as a particular net proton fraction. We denote the density at which the two-phase equilibrium ceases to have a lower energy per particle than the uniform phase by $n_{1\rightarrow 2}$. The values of $n_{\mathrm{p-drip}}$ and $n_{1\rightarrow 2}$ for the interactions we examine are listed in Table 1.

To be concrete, consider the situation at a pressure of 0.503 MeV·fm^{-3}, shown as a fragment of an isobar in the main part of Fig. 7, and also in the inset. One can see that it is possible to have equal pressures, neutron chemical potentials *and* proton chemical potentials for a $\sim 5\%$ solution of protons in neutrons, and a vanishingly small solution of protons in neutrons. For a pressure of 0.538 MeV·fm^{-3}, shown also in the inset on Fig. 7, there is coexistence between a $\sim 4\%$ solution of protons, and one with

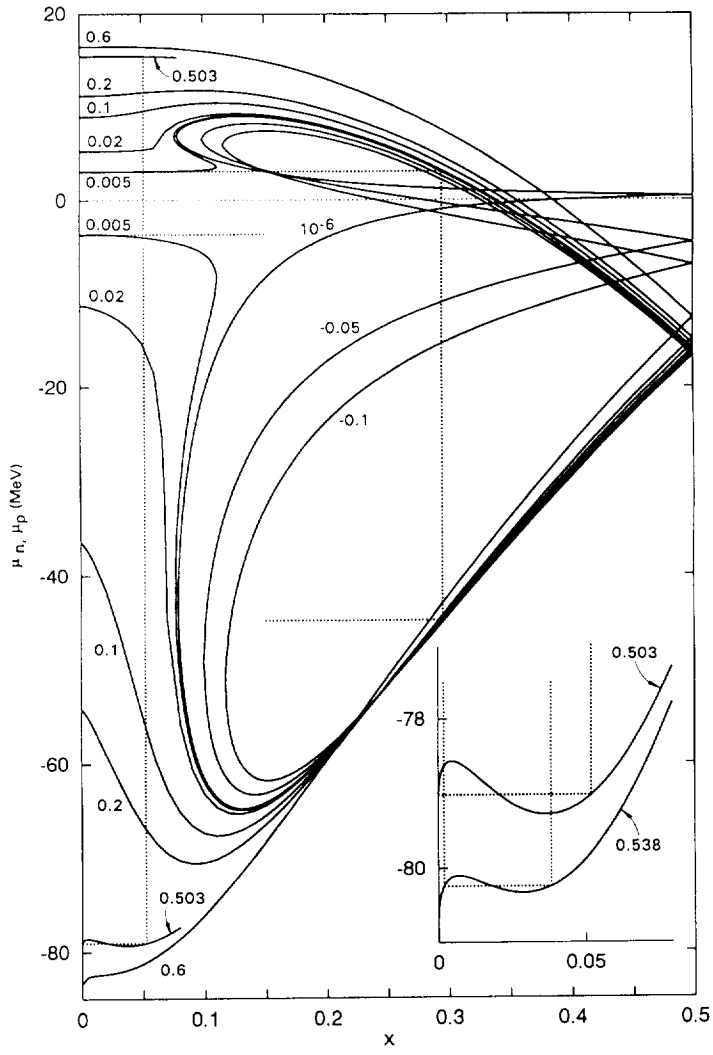

Fig. 7. Nuclear pressure isobars on a pn chemical potential versus proton-fraction plot. The interaction used is FPS21 (see text). The pressure values listed are in MeV·fm^{-3}. The vertical and horizontal lines on the main figure locate the pure neutron and nuclear fluid phases that are in thermodynamic equilibrium. The isobars involved are p = 0.005 MeV·fm^{-3} (just beyond neutron drip) and p = 0.503 MeV·fm^{-3} (the onset of proton drip). Inset are enlarged views of μ_p for the latter case (upper curve), and for p = 0.538 MeV·fm^{-3}, the limit of two-fluid equilibrium where both fluids have non-zero proton fractions (lower curve).

$\sim 0.2\%$. Some properties of the matter as a function of density are shown in Fig. 8. The fraction $X_{\rm nuc}$ of matter in the "nuclear" component climbs steadily with density, and has reached 0.71 at $n_{\rm p-drip}$. The proton fraction of this component, $x_{\rm nuc}$, falls steadily, while that of the neutron component, $x_{\rm drip}$, is of course zero. As the density increases beyond $n_{\rm p-drip}$, the properties of the "nuclear" component continue changing as before,

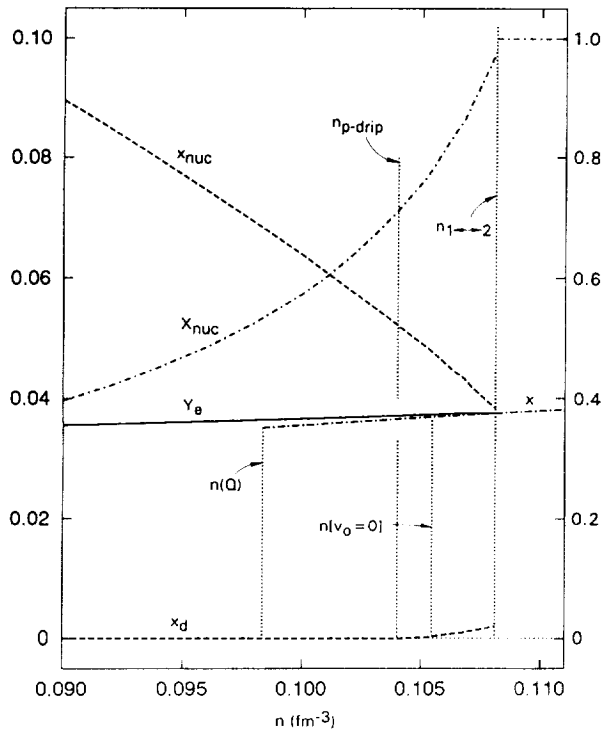

Fig. 8. Some properties of the two-fluid approximation to nuclear matter, as functions of density, and its connection to the interior nuclear liquid. For the two-fluid case they are the charge fractions x_{nuc} of the "nuclear" component, and x_{drip} of the nominally neutron component, the net charge fraction Y_e, and the mass fraction X_{nuc} in the nuclear component. At the right side the matter becomes one uniform nuclear fluid, which has $X_{nuc} = 1$ and proton fraction x. The densities $n(Q)$, $n[v_Q = 0]$, the proton-drip density n_{p-drip} and the phase-transition density $n_{1\leftrightarrow 2}$ are discussed in the text.

but x_{drip} now becomes non-zero. At a density of $n_{1\leftrightarrow 2}$, the phase transition density, X_{nuc}, achieves the value unity, the "drip" component has disappeared, and the nuclear component becomes the one-uniform-fluid phase of the neutron-star interior. Over this small density range, the dripped proton fraction increases as the density increases, just as it does with neutron drip in nuclei at much lower densities, but the actual fraction of matter in that component decreases, going to zero at the phase transition.

So far as Fig. 7 is concerned, the mechanism is as follows. As is seen most clearly in the inset to Fig. 7, $\mu_p(x, p)$ does not approach the value $x = 0$ smoothly, but has a cusp there. This behavior is due to the proton kinetic energy contribution to μ_p, which is proportional to $x^{2/3}$. If the pressure is increased slightly from the proton-drip value, the μ_p isobar is lowered at very small x, and phase equilibrium may be maintained by having a finite, but small, proton concentration in the (nominally) neutron-fluid part of the two-fluid system. The lower curve of the inset to Fig. 7 corresponds to the phase transition to uniform matter. The possibility of the further rise of μ_p provides a tiny region of metastability of the two-fluid phase above this transition density. The

corresponding metastability of the one-fluid phase at densities below $n_{1\leftrightarrow 2}$ is actually bounded by the instability density $n(Q)$ discussed earlier. Within the limitations of the model we are using in this section, however, with no gradient or Coulomb contributions, that bound on the density would become $n[v_0 = 0] = 0.1055\ \mathrm{fm}^{-3}$, as given by Eq. (6). Both density limits are shown in Fig. 8.

To summarize, the density $n_{\mathrm{p-drip}}$ is not an instability, but signals the onset of a modified two-fluid phase. It occurs for all four of the effective interactions we have studied, but its occurrence requires a rather intricate coupling between the behavior of μ_{p} and μ_{n} at low proton fraction, so that it is not clear that it occurs for all effective interactions. Either $n_{\mathrm{p-drip}}$, if it occurs, or $n_{1\leftrightarrow 2}$ can be used as an indicator of the proximity of the solid-to-liquid transition.

The actual phase boundary between the solid phase and the uniform phase is modified by the Coulomb and surface contributions that a more complete calculation of the solid phase [10] gives. As shown in the previous section, the density $n(Q)$, which contains gradient and Coulomb contributions, is a good approximation to the phase boundary. The densities discussed in this section, especially $n_{1\leftrightarrow 2}$, provide a rather simple alternative way to gauge the properties of any given interaction. As discussed above, $n_{1\leftrightarrow 2}$ must always be greater than $n_{\mathrm{p-drip}}$, a condition that Table 1 confirms. Since it lacks gradient and Coulomb terms, which constitute positive contributions to the energy, it must be an upper limit to the phase boundary.

The densities $n(Q)$ and $n_{\mathrm{p-drip}}$, which are properties of different phases of the matter, may occur in either order, although in the cases we document in Table 1 $n(Q)$ is always the smaller of the two. An interesting question that these considerations raise is whether the detailed calculations for inhomogeneous systems give a higher transition density if the possibility of proton drip is included. That question is deferred for future work.

8. Discussion

We have examined the stability against inhomogeneity of beta-stable matter, as an indicator of the solid-to-liquid phase transition that occurs at the inner boundary of the solid crust of a neutron star. In particular, we have found that the interactions that possess neutron-matter properties in agreement with the microscopic calculations of Pandharipande and coworkers [13,16] also give relatively high densities ($n \sim 0.1\ \mathrm{fm}^{-3}$) for the stability limit of the high-density, uniform phase. Such a high instability limit allows a larger density range for the various non-spherical solid phases, with important consequences for crustal properties of neutron stars. We now examine some more recent microscopic calculations, to explore the extent of the agreement with those we have relied on.

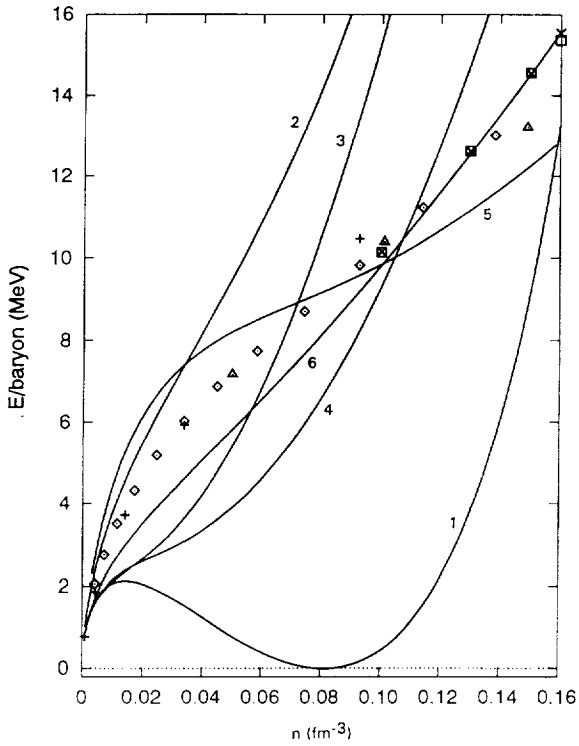

Fig. 9. The energy per baryon of uniform neutron matter as a function of density, a comparison with other microscopic calculations and various other effective interactions. Results from microscopic calculations are represented with data points: the diamonds are the values obtained using the V14 potential plus a three-nucleon interaction, from Ref. [13], the "+" signs using the Reid potential, from Ref. [16]. The triangles are non-relativistic calculations using the Bonn-A potential, from Ref. [26]. The squares and crosses are relativistic calculations using the Bonn-A potential, from Refs. [25,26], the two sets of values being too close to distinguish in the figure for most of the density range. The full curves come from effective interactions mentioned in the discussion section: the curve labelled (1) is from Ref. [27]; (2) and (3) are from Ref. [28], (2) having only linear terms in the σ-field, (3) having non-linear terms; (4) is from Ref. [30]; (5) is based on Ref. [31], using the parameter set corresponding to a nuclear incompressibility of $K = 200$ MeV; (6) is SkM*, a modified version [29] of SkM.

8.1. Observations

We recall that Ref. [13] uses the V14 two-body potential plus a three-nucleon interaction, and Ref. [16] uses the Reid potential. Recent calculations by Li et al. [25] and by Bao et al. [26] use the Bonn-A potential and relativistic Dirac–Brueckner many-body theory. The latter reference [26] includes also non-relativistic Brueckner–Hartree–Fock treatments of that potential. At the few densities that fall in our range of interest, their results are in excellent agreement with those of Ref. [13], as is shown in Fig. 9. It is tempting to believe that at densities below 0.1 fm^{-3} the energy per baryon of neutron matter calculated ab initio constitutes well-determined "data". For the convenience of other workers, numerical values for the points plotted in Fig. 9 are given in Table 5.

Table 5
Numerical values used in Fig. 9 of the energy per baryon $\mathcal{E}$ of neutron matter, and other quantities when given, as a function of density

n (fm^{-3})	$\mathcal{E}$ (MeV)	μ_n (MeV)	p (MeV·fm^{-3})
0.000912 [a]	0.78	−3.19	
0.00422 [a]	1.86	−9.09	
0.01425 [a]	3.71	−19.23	
0.03377 [a]	5.93	−33.83	
0.0927 [a]	10.46	−64.3	
0.1659 [a]	16.	−88.4	
0.004222 [b]	2.057		0.004517
0.007295 [b]	2.747		0.01065
0.01153 [b]	3.503		0.02115
0.01729 [b]	4.322		0.03871
0.02462 [b]	5.177		0.06331
0.03377 [b]	6.027		0.09506
0.04495 [b]	6.873		0.1402
0.05836 [b]	7.744		0.2101
0.07420 [b]	8.699		0.3287
0.09267 [b]	9.822		0.5375
0.1140 [b]	11.22		0.8977
0.1383 [b]	13.01		1.473
0.1659 [b]	15.26		2.408
0.050 [c]	7.164		
0.101 [c]	10.384		
0.149 [c]	13.209		
0.169 [c]	14.432		
0.10 [d]	10.14		
0.13 [d]	12.62		
0.15 [d]	14.56		
0.16 [d]	15.37		
0.10 [e]	10.15		
0.13 [e]	12.62		
0.15 [e]	14.55		
0.16 [e]	15.54		

[a] From Siemens and Pandharipande, Ref. [16].
[b] From Friedman and Pandharipande, Ref. [13].
[c] Non-relativistic, from Bao et al., Ref. [26].
[d] Relativistic, from Bao et al., Ref. [26].
[e] From Li et al., Ref. [25].

Nuclear theories intended for the dense neutron-star interior may not be able to give a good description of the crust region, and perhaps that deficiency is not relevant to their purpose. On the other hand, the fitting of such models to neutron-matter "data" may provide a useful constraint on parameters of the model. To illustrate the extent of possible departures from the microscopic "data" on neutron matter, we include in Fig. 9 the energy per baryon, as a function of density, for some popular effective-interaction models. The Walecka relativistic mean-field model, as presented by Serot [27], and labelled "1" in the figure, departs markedly from the "data" in the low-density regions,

and even predicts a neutron-matter bound state. In a more complex form more adaptable to the isospin flexibility needed, two versions of this model described by Reinhard et al. [28] are also illustrated in Fig. 9. One labelled "2" has a linear σ-field, the other, "3", a non-linear one. It should be emphasized that, so far as we know, no attempt has been made to adjust these models to neutron-matter properties. It seems likely, from the three RMF curves shown, that the more complex model possesses sufficient flexibility for a better fit to be achieved. The neutron-matter properties they predict at higher densities would clearly be much changed by such a modification.

To continue the comparisons, we include in Fig. 9 some non-relativistic model results. The curve labelled "6" is the Skyrme interaction SkM* now used in preference to SkM by Bonche and coworkers [29] [3], which has slightly modified values of t_1 and t_2, and its energy thus departs a little from that of SkM at the higher densities. The density for instability against proton clumping, $n(Q)$, is increased from that of SkM, illustrated in Fig. 3, by only about 0.001 fm^{-3}. It is thus unlikely that neutron-star results obtained using SkM [10] will be significantly modified by the use of SkM*.

Some other non-relativistic models that have been used extensively for studying properties of terrestrial nuclei, and whose predictions for neutron-star crusts would be interesting to have, were the models suitably modified, are also shown in Fig. 9. The model of Myers et al. [30], "4", uses a classical two-body interaction fitted extensively to stability-line nuclei. The model of Fayans and co-workers [31], "5", treats in mean-field approximation a finite-range effective interaction adjusted to match nuclear ground-state and excited state properties. In each case there is considerable departure of the predictions from the neutron-matter "data", as is to be expected with so large an extrapolation in proton fraction from the valley of stability. With the interaction of Ref. [31], for example, it is not difficult, by adjusting only two of the parameters of the model [32] [4], to match the neutron "data" closely in the density range considered here. Such a modification then necessitates readjustment of the fit to properties of nuclei, of course. One may hope that fitting neutron-matter properties, given the large "lever arm" in proton fraction that is involved, will also have a beneficial effect on the ability of models to match properties of nuclei further from the stability line.

For the sake of brevity we have not included plots of pressure and chemical potentials for these other interactions. In general, since those quantities involve derivatives of the energy, the departures among the models that is seen, and the differences from a model such as FPS21 that they show, are relatively larger than for the energy. In order that the stability properties, which involve these derivative quantities, are well determined, it is important to achieve a close fit to the energy as a function of density.

[3] We thank Dr. E. Chabanat for providing us the parameter values of Skm*.

[4] We thank Dr. Fayans for providing us with a program that applies that interaction to uniform matter.

8.2. Suggestions

To the extent that there exist microscopic calculations of neutron-matter properties that are unanimous, it seems to us highly desirable that effective hamiltonians proposed for the density range $n \lesssim n_s$, and even those intended for higher densities, should be adjusted to fit closely those properties.

The crucial role that ab initio microscopic calculations play in this problem is clear. The agreement between Refs. [13,16] on the neutron-matter energy per baryon, obtained using different potentials and different many-body techniques, extends up to $n_n \sim 0.05$ fm^{-3}, and that between Refs. [13,25,26], again with different potentials and different many-body techniques, improves the agreement to $n_n \lesssim 0.1$ fm^{-3}. It would be invaluable for the proponents of other microscopic two-nucleon interactions to calculate neutron-matter properties at densities $\lesssim 0.1$ fm^{-3}, since these properties are a vital, but experimentally inaccessible, input to the elucidation of neutron-star structure.

We hope to have made evident that other quantities besides the energy of neutron matter are needed to substantiate or improve the assumptions implicit in most effective interactions:

The instability analysis needs the proton chemical potential μ_p and its density derivatives for beta-stable matter. (All other explorations of the crust phase boundary use information equivalent to this.) Direct many-body calculations of μ_p for neutron matter, a simpler task than for matter of arbitrary charge state, would provide a more accurate value, and avoid reliance on the quadratic charge-symmetry expansion around nuclear matter that effective interactions are forced to assume.

Crucial to the location of the instability density are the gradient terms in the effective hamiltonian. The present work neglects possible spin-exchange contributions to the t_1 and t_2 terms of the Skyrme t-matrix. The presence of such contributions would modify the gradient terms, and thus the phase boundary. The possible presence of spin exchange needs in microscopic calculations consideration of spin-non-saturated systems, as can be seen from the last lines of Eq. (A.2). There may be alternative approaches to obtaining these gradient terms, but information about them in some form from microscopic calculations is very desirable.

8.3. Skyrme-like interactions and neutron potentials

We return to a point discussed in an earlier section concerning the behavior of the generalized Skyrme interactions at low density [5]. We show in Fig. 10 the behavior of a quantity $T(n)$ related to the potential-energy part of the energy per baryon $\varepsilon = E/n$ for neutron matter:

$$T(n) = \frac{1}{n}\left(\varepsilon - \frac{3}{5}\frac{\hbar^2 k_F^2}{2m}\right). \tag{11}$$

[5] This section owes much to V.R. Pandharipande. We hope to pursue its implications with him in the future.

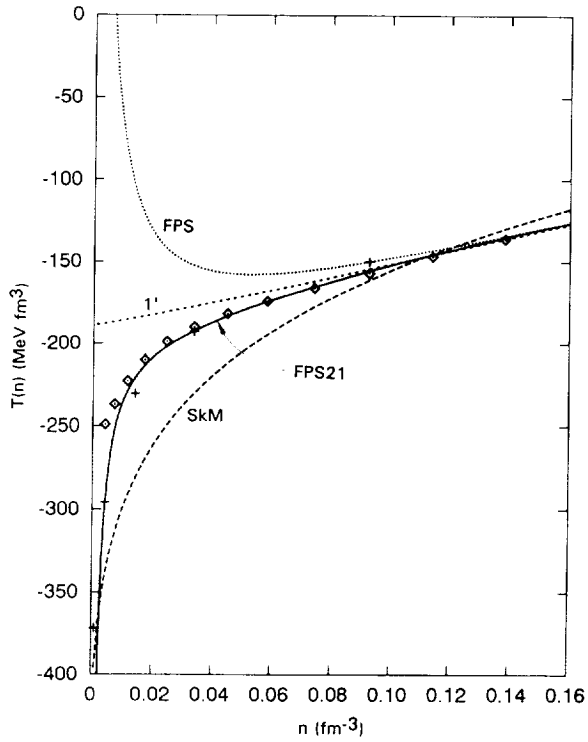

Fig. 10. The neutron potential-energy-related quantity $T(n)$, (11), as a function of neutron density. The diamonds are the values obtained by Friedman and Pandharipande [13] the "+" signs those of Siemens and Pandharipande [16] The interactions Skyrme 1′, SkM, FPS and FPS21 are described in the text.

For the customary Skyrme interactions,

$$T(n) \to \tfrac{1}{4}t_0(1 - x_0), \qquad n \to 0 \qquad \text{(Skyrme)}. \tag{12}$$

For Skyrme 1′ and SkM, that is the behavior exhibited; the linear rise in the former case is due to its t_3 term, since for it $\alpha = 1$. The behavior of the other interactions is directly traceable to their parameter values, which are given in the tables. On the other hand, for a dilute neutron gas with scattering length $-|a|$, the behavior at low densities given by many-body theory is (see for example Ref. [33])

$$\begin{aligned} T(n) &= -\frac{\hbar^2\pi|a|}{m}\left(1 - \frac{6}{35\pi}(11 - 2\ln 2)k_F|a| + \cdots\right), \\ &\simeq -2480\ \text{MeV}\cdot\text{fm}^3(1 - 0.525k_F|a|). \end{aligned} \tag{13}$$

where the numerical values result from taking a nn scattering length $|a| = 19$ fm. With that value, the quantity $k_F|a|$ in the expansion of (13) is unity at a neutron-matter density of $n_{|a|} = 0.49 \times 10^{-5}$ fm^{-3}. This is too small a density for the behavior given by (13) to be visible in Fig. 10, or to be an accurate approximation even at the lowest densities used in the ab initio calculations. But clearly the energies obtained by Refs. [16,13] exhibit

the right tendency, in that $T(n = 0) = -2480$ MeV·fm^3, far below the values shown in Fig. 10. The figure shows that FPS21 qualitatively shares that property, although its singular behavior at $n_n = 0$ would need slight modification to match Eq. (13).

The rather large variations in behavior of the four effective interactions at very low density is masked in the equation of state by the kinetic-energy contribution, so that the presence of a term $\propto n$ in E is not the ingredient that determines the behavior of neutron-star matter in the density range 0.05 fm^{-3} $< n <$ 0.1 fm^{-3}. (The fact that FPS and Skyrme t′ agree well with FPS21 so far as the instability criteria are concerned is proof of this point.) But in the Hartree–Fock single-neutron potential, such a term would contribute a constant, *density-independent*, attractive potential at very low neutron density. The correct matching to the "data" of Refs. [13,16]) and to the theory of Eq. (13) will cause the potential to eventually $\rightarrow 0$ at neutron densities $\lesssim n_{|a|}$, of course. But such a contribution, which does not arise with the usual Skyrme parametrizations (although it could be introduced), may have implications for neutron "haloes" in very neutron-rich nuclei.

9. Conclusion

Earlier results on the density of the solid–liquid phase boundary in dense neutron-star matter ranged from 0.03 fm^{-3} of Refs. [2,3] to 0.17 fm^{-3} of Ref. [4]. The study that fitted neutron matter to what we have used as one of our standards [16] Ref. [5], obtained a density of 0.09 fm^{-3}. That already was an indication that the properties ascribed to neutron matter have an important effect on the density obtained for this phase transition. The interaction FPS21 introduced in the present work is a close fit to more recent neutron-matter energies [13] and, as shown in Table 1, it gives for the density of the onset of proton clustering the value $n(Q) \simeq 0.0983$ fm^{-3}. This we estimate to be $\lesssim 0.001$ fm^{-3} less than the density of the solid-liquid phase boundary. The value of the transition *density* determines the structure of the inner part of the crust: if it is sufficiently high, it is possible for non-spherical phases, with rod- or plate-like nuclei, to occur before the nuclei dissolve. This happens for the interactions FPS21, FPS and Skyrme t′. If it is relatively low, as occurs for SkM, then the matter makes a direct transition from spherical nuclei to uniform nucleon fluid. The extent to which the non-spherical phases occur will have important consequences, we believe, for other neutron-star properties that are determined in the crust.

For a thin crust, in the plane approximation, the crust *mass*, and thus the crust moment of inertia, are proportional to the matter *pressure* at the phase transition. An explicit formula for the crust mass in terms of this pressure, and the neutron-star mass and radius, is given in Ref. [10]. For different interactions the pressure–density relationship may vary, especially for interactions that do not fit the neutron-matter properties [13] closely. For example, as is seen in Table 1, the transition pressure obtained for SkM is slightly greater than that given by FPS, even though its transition density is considerably lower. (For Ref. [5] the pressure we obtain at the density quoted above is 0.47 MeV·fm^{-3},

closer than any of our other results to that of FPS21.)

For the interaction FPS21, the value of the matter pressure at the crust boundary, given in Table 1, is 0.500 MeV·fm^{-3}. This is $\sim 30\%$ greater than for FPS. If the value of the moment of inertia of the crust relative to the total moment for the FPS interaction, taken from Table 1 of Ref. [10], is scaled according to the boundary pressures of FPS21 and FPS, one obtains the value $\Delta I_c/I = 2.6\%$. (That quantity depends on the mass and radius of the star, of course, and the values illustrated were for a neutron star of mass $1.445 M_\odot$ and radius 10.79 km. The approximate dependence of the relative crust moment of inertia on mass and radius is given in Ref. [34].) This value of $\Delta I_c/I$ is, perhaps fortuitously, identical with that obtained from the glitch analysis of Chau et al. [35] Detailed calculations of the equation of state with the interaction FPS21, and application to neutron-star models, have yet to be done, however.

Acknowledgements

We thank Vijay Pandharipande for many useful discussions and suggestions. Conversations with Hoi-Fung Chau have been very helpful. We thank Jochen Wambach for sharing his program of the interaction of Fayans et al., Morten Hjorth-Jensen for data concerning the Oslo–Trondheim equation-of-state calculations [26] and John W. Clark and Andrew D. Jackson for helpful correspondence. This work was supported in part by the U.S. National Science Foundation under grants NSF PHY 89-21025, NSF PHY 91-00283 and NSF AST93-15133, and by NASA under grant NAGW-1583.

Appendix. Skyrme and Skyrme-like interactions

To illustrate comments made in the text, we include here all of the spin-exchange terms in the t-matrix:

$$t(\boldsymbol{k},\boldsymbol{k}') = \tfrac{1}{2}t_1(1+x_1P_\sigma)(k^2+k'^2) + t_2(1+x_2P_\sigma)\boldsymbol{k}\cdot\boldsymbol{k}' + t_0(1+x_0P_\sigma) + t_3(1+x_3P_\sigma)n^{2+\alpha}, \tag{A.1}$$

With the assumption that t_i and x_i are constant, this t-matrix produces a hamiltonian density of the form

$$H = \left(\frac{\hbar^2}{2m} + \tfrac{1}{4}\left[t_1(1+\tfrac{1}{2}x_1) + t_2(1+\tfrac{1}{2}x_2)\right]n - \tfrac{1}{4}\left[t_1(\tfrac{1}{2}+x_1) - t_2(\tfrac{1}{2}+x_2)\right]n_n\right)\tau_n + \left(\frac{\hbar^2}{2m} + \tfrac{1}{4}\left[t_1(1+\tfrac{1}{2}x_1) + t_2(1+\tfrac{1}{2}x_2)\right]n\right.$$

$$
\begin{aligned}
&-\tfrac{1}{4}\left[t_1(\tfrac{1}{2}+x_1)-t_2(\tfrac{1}{2}+x_2)\right]n_{\rm p}\Big)\tau_{\rm p}\\
&+\tfrac{1}{2}t_0\left((1+\tfrac{1}{2}x_0)n^2-(\tfrac{1}{2}+x_0)(n_{\rm n}^2+n_{\rm p}^2)\right)\\
&+\tfrac{1}{12}t_3\left((1+\tfrac{1}{2}x_3)n^2-(\tfrac{1}{2}+x_3)(n_{\rm n}^2+n_{\rm p}^2)\right)n^{\alpha}\\
&-\tfrac{1}{16}\left[3t_1(1+\tfrac{1}{2}x_1)-t_2(1+\tfrac{1}{2}x_2)\right]n\nabla^2 n\\
&+\tfrac{1}{16}\left[3t_1(\tfrac{1}{2}+x_1)+t_2(\tfrac{1}{2}+x_2)\right](n_{\rm n}\nabla^2 n_{\rm n}+n_{\rm p}\nabla^2 n_{\rm p})\\
&-\tfrac{1}{16}(t_1x_1+t_2x_2)\boldsymbol{J}^2+\tfrac{1}{16}(t_1-t_2)(\boldsymbol{J}_{\rm n}^2+\boldsymbol{J}_{\rm p}^2).
\end{aligned}
\tag{A.2}
$$

where $n_{\rm n}$, $n_{\rm p}$ are neutron and proton densities, $n=n_{\rm n}+n_{\rm p}$, $\tau_{\rm n}$ and $\tau_{\rm p}$ are kinetic densities and $\boldsymbol{J}_{\rm n}$ and $\boldsymbol{J}_{\rm p}$ are spin densities [14,36]. The interactions of this form that we quote in the text have the parameter values given in Table 2, and all have $x_1=x_2=0$.

In the generalized Skyrme interactions that have been constructed to give nuclear and neutron matter that matches the numerical results of Ref. [13], the effective t-matrix elements have a density dependence, so that the hamiltonian density for uniform matter becomes

$$
\begin{aligned}
H=&\left(\frac{\hbar^2}{2m}+(p_3n+p_5n_{\rm n})\,{\rm e}^{-p_4n}\right)\tau_{\rm n}+\left(\frac{\hbar^2}{2m}+(p_3n+p_5n_{\rm p})\,{\rm e}^{-p_4n}\right)\tau_{\rm p}\\
&-n^2\left[p_1\,{\rm e}^{-p_6n}+p_2(1-{\rm e}^{-p_6})+\left(\frac{p_{10}}{n}+p_{11}\right){\rm e}^{-(p_9n)^2}\right]\\
&-\tfrac{1}{4}(n_{\rm n}-n_{\rm p})^2\left[p_7\,{\rm e}^{-p_6n}+p_8(1-{\rm e}^{-p_6n})+\left(\frac{p_{12}}{n}+p_{13}\right){\rm e}^{-(p_9n)^2}\right]\\
&+H_{\rm gradient}.
\end{aligned}
\tag{A.3}
$$

At a given density $n_{\rm n,p}$, the kinetic densities $\tau_{\rm n,p}$ depend on the temperature. The τ-dependent terms are fitted to the finite-temperature energies of nuclear and neutron matter, and then the potential-energy terms may be fitted by comparison with the zero-temperature energies. The particular form of the density dependence of the potential energy in (A.3) made the fitting to nuclear matter ($n_{\rm n}=n_{\rm p}$) and then to neutron matter somewhat easier. The relationship $(n_{\rm n}-n_{\rm p})^2=2(n_{\rm n}^2+n_{\rm p}^2)-n^2$ makes clear the connection between (A.2) and (A.3). The parameter values that achieve the fit to the ab initio microscopic calculations of Ref. [13] are shown in Table 3.

For the gradient terms of the generalized Skyrme interaction it is convenient to adopt a different notation. If the parameters in the t-matrix (A.1) become functions of the total density n, then we define the combinations that occur in the kinetic part of the hamiltonian as

$$
\mathcal{P}_i(n)=\tfrac{1}{4}t_i(n)(1+\tfrac{1}{2}x_i(n)),\qquad \mathcal{Q}_i(n)=\tfrac{1}{4}t_i(n)(\tfrac{1}{2}+x_i(n)),\quad i=1,2,
\tag{A.4}
$$

so that the kinetic part of the hamiltonian has the form

$$
H_{\rm kin}=\sum_{t={\rm n,p}}\left(\frac{\hbar^2}{2m}+[\,\mathcal{P}_1(n)+\mathcal{P}_2(n)\,]\,n-[\,\mathcal{Q}_1(n)-\mathcal{Q}_2(n)\,]\,n_t\right)\tau_t.
\tag{A.5}
$$

With the supplementary definitions

$$\mathcal{P}_{i;\mathrm{f}}(n) = \frac{1}{n}\int_0^n \mathcal{P}_i(n')\,\mathrm{d}n', \qquad \mathcal{Q}_{i;\mathrm{f}}(n) = \frac{1}{n}\int_0^n \mathcal{Q}_i(n')\,\mathrm{d}n', \tag{A.6}$$

the gradient contributions to the hamiltonian are

$$\begin{aligned} H_{\mathrm{gradient}} = &-\tfrac{1}{4}(2\mathcal{P}_1 + \mathcal{P}_{1;\mathrm{f}} - \mathcal{P}_{2;\mathrm{f}})n\nabla^2 n + \tfrac{1}{2}(\mathcal{Q}_1 + \mathcal{Q}_2)(n_\mathrm{n}\nabla^2 n_\mathrm{n} + n_\mathrm{p}\nabla^2 n_\mathrm{p}) \\ &-\tfrac{1}{4}(\mathcal{Q}_1 - \mathcal{Q}_2)([\nabla n_\mathrm{n}]^2 + [\nabla n_\mathrm{p}]^2) + \frac{1}{2}\frac{\partial \mathcal{Q}_2}{\partial n}(n_\mathrm{n}\nabla n_\mathrm{n} + n_\mathrm{p}\nabla n_\mathrm{p})\cdot\nabla n. \end{aligned} \tag{A.7}$$

This expression reduces to that of Ref. [36] for the special case of at most linear dependence on n of the parameters in (A.1). The restricted parametrization employed in the body of this paper assumes that x_1 and x_2 are zero, so that $\mathcal{Q}_i = \frac{1}{2}\mathcal{P}_i$, and

$$\mathcal{P}_1 = (\tfrac{1}{2}p_3 - p_5)\,\mathrm{e}^{-p_4 n}, \qquad \mathcal{P}_2 = (\tfrac{1}{2}p_3 + p_5)\,\mathrm{e}^{-p_4 n}, \tag{A.8}$$

in terms of the parameters used in (A.3).

References

[1] M.A. Alpar, H.F. Chau, K.S. Cheng and D. Pines, Astrophys. J. 409 (1993) 345.
[2] W.D. Langer, L.C. Rosen, J.M. Cohen and A.G.W. Cameron, Astrophys. Space Sci. 5 (1969) 529.
[3] H.A. Bethe, G. Börner and K. Sato, Astron. Astrophys. 7 (1970) 279.
[4] G. Baym, H.A. Bethe and C.J. Pethick, Nucl. Phys. A 175 (1971) 225.
[5] J. Arponen, Nucl. Phys. A 191 (1972) 257.
[6] J.R. Buchler and Z. Barkat, Phys. Rev. Lett. 27 (1971) 48.
[7] J.S. Levinger and L.M. Simmons, Phys. Rev. 124 (1961) 916.
[8] J. Nemeth and D.W.L. Sprung, Phys. Rev. 176 (1968) 1496
[9] K. Oyamatsu, Nucl. Phys. A 561 (1993) 431.
[10] C.P. Lorenz, D.G. Ravenhall and C.J. Pethick, Phys. Rev. Lett. 70 (1993) 379; C.P. Lorenz, Ph.D Thesis, Univ. of Illinois (1991) (unpublished).
[11] C.J. Pethick, D.G. Ravenhall and J.M. Lattimer, Nucl. Phys. A 414 (1984) 517.
[12] L. Mirsky, An introduction to linear algebra (Clarendon, Oxford, 1955) Section 13.3.
[13] B. Friedman and V.R. Pandharipande, Nucl. Phys. A 361 (1981) 502.
[14] D. Vautherin and D.M. Brink, Phys. Rev. C 5 (1972) 626.
[15] M. Brack, B.K. Jennings and Y.H. Chu, Phys. Lett. B 65 (1976) 1.
[16] P.J. Siemens and V.R. Pandharipande, Nucl. Phys. A 173 (1971) 561.
[17] D.G. Ravenhall, C.D. Bennett and C.J. Pethick, Phys. Rev. Lett. 28 (1972) 978.
[18] J.M. Lattimer, C.J. Pethick, D.G. Ravenhall and D.Q. Lamb, Nucl. Phys. A 432 (1985) 646.
[19] H. Krivine, J. Treiner and O. Bohigas, Nucl. Phys. A 336 (1980) 155.
[20] P. Bonche and D. Vautherin, Nucl. Phys. A 372 (1981) 496; Astron. Astrophys. 112 (1982) 268.
[21] M. Lassaut, H. Flocard, P. Bonche, P.H. Heenen and E. Suraud, Astron. Astrophys. 183 (1987) L3.
[22] V.R. Pandharipande and D.G. Ravenhall, Proc. NATO Advanced Research Workshop on nuclear matter and heavy ion collisions, Les Houches, 1989, eds. M. Soyeur et al. (Plenum, New York, 1989) p. 103.
[23] D.G. Ravenhall, unpublished calculations (1994).
[24] I.E. Lagaris and V.R. Pandharipande, Nucl. Phys. A 369 (1981) 470.
[25] G.Q. Li, R. Machleidt and R. Brockmann, Phys. Rev. C 45 (1992) 2782.
[26] G. Bao, L. Engvik, M. Hjorth-Jensen, E. Osnes and E. Østgaard, preprint (1993); M. Hjorth-Jensen, private communications (1994).

[27] B.D. Serot, Rep. Prog. Phys. 55 (1992) 1855.
[28] P.-G. Reinhard, M. Rufa, J. Maruhn, W. Greiner and J. Friedrich, Z. Phys. A 323 (1986) 13.
[29] J. Skalski, Ph. Heenen and P. Bonche, Nucl. Phys. A 559 (1993) 221.
[30] W.D. Myers, W.J. Swiatecki and C.S. Wang, Nucl. Phys. A 436 (1985) 185.
[31] S.A. Fayans, E.L. Trykov and D. Zawischa, Nucl. Phys. A 568 (1994) 523.
[32] J. Wambach and D.G. Ravenhall, unpublished calculations (1994).
[33] A.L. Fetter and J.D. Walecka, Quantum theory of many-particle systems (McGraw-Hill, New York, 1971) p. 149.
[34] D.G. Ravenhall and C.J. Pethick, Astrophys. J. 424 (1994) 846.
[35] H.F. Chau, P.M. McCulloch, R. Nandkumar and D. Pines, Astrophys. J. 413 (1993) L113.
[36] S. Krewald, V. Klempt, J. Speth and A. Faessler, Nucl. Phys. A 281 (1977) 166.

LaTeX. Papers that have been accepted for publication may be sent as an electronic file to the Publisher by e-mail or on a diskette (allowed formats are 3.5" or 5.25" MS-DOS, or 3.5" Macintosh). If the electronic file is suitable for processing by the Publisher, proofs will be produced without rekeying the full text. The article should be encoded in ESP-LaTeX, in standard LaTeX (in document style article) or in REVTeX. The authors should include an ASCII table (available from the Publisher) in their files, to enable any transmission errors to be detected. The ESP-LaTeX package (including detailed instructions) can be obtained using anonymous ftp from the Comprehensive TeX Archive Network;

Host name	*CTAN directory*
ftp.dante.de	/pub/tex/macros/latex/contrib/elsevier
ftp.tex.ac.uk	/pub/archive/macros/latex/contrib/elsevier
ftp.shsu.edu	/tex-archive/macros/latex/contrib/elsevier

The files, as well as instructions in the form of a booklet, can also be obtained from the Publisher.

No changes from the version accepted by the Editorial Office of the journal are permissible, without prior and explicit approval.

The Publisher reserves the right to decide whether to process a manuscript from the authors' file or not. Files coded in a simple and consistent manner are most likely to be used for production.

Unless requested explicitly, no proofs will be sent to the author if the paper is processed from the authors' file.

Proofs. Proofs will usually be printed on low-quality paper. Proofs will be sent to the author 4–6 weeks after acceptance. Please note that the proofs have been proofread by the Publisher and only a cursory check by the author is needed; we are unable to accept changes in, or additions to, the edited manuscript at this stage. In order to guarantee the fastest possible production times, the proofs must be returned within 48 hours of receipt, preferably by fax. If no reply is received from the author, the Publisher assumes that there are no further corrections to be made and will proceed with publication of the article.

Colour plates. Illustrations can be printed in colour when they are judged by the Editor to be essential to the presentation. The Publisher and the author will each bear part of the extra costs involved. Further information concerning colour illustrations and the cost to the author is available from the Publisher.

Nuclear Physics A (ISSN 0375-9474). For 1995, volumes 581–595 are scheduled for publication. Subscription prices are available upon request from the Publisher. A combined subscription to Nuclear Physics A volumes 581–595, Nuclear Physics B volumes 433–457, and Nuclear Physics B Proceedings Supplements volumes 39–44 is available at a reduced rate.

Subscriptions are accepted on a prepaid basis only and entered on a calendar year basis. Issues are sent by surface mail except to the following countries where air delivery via SAL is ensured: Argentina, Australia, Brazil, Canada, P.R. China, Hong Kong, India, Israel, Japan, Malaysia, Mexico, New Zealand, Pakistan, Singapore, South Africa, South Korea, Taiwan, Thailand, USA. For all other countries airmail rates are available upon request.

Please address all your requests regarding orders and subscription queries to: Elsevier Science B.V., Journal Department, P.O. Box 211, 1000 AE Amsterdam, The Netherlands; telephone: +31 20 4853642; fax: +31 20 4853598. Claims for issues not received should be made within six months of our publication (mailing) date.